Temperature responses to spectral solar variability on decadal time scales

Robert F. Cahalan,[1] Guoyong Wen,[1,2] Jerald W. Harder,[3] and Peter Pilewskie[3]

Received 1 December 2009; revised 24 February 2010; accepted 1 March 2010; published 6 April 2010.

[1] Two scenarios of spectral solar forcing, namely Spectral Irradiance Monitor (SIM)-based out-of-phase variations and conventional in-phase variations, are input to a time-dependent radiative-convective model (RCM), and to the GISS modelE. Both scenarios and models give maximum temperature responses in the upper stratosphere, decreasing to the surface. Upper stratospheric peak-to-peak responses to out-of-phase forcing are ~0.6 K and ~0.9 K in RCM and modelE, ~5 times larger than responses to in-phase forcing. Stratospheric responses are in-phase with TSI and UV variations, and resemble HALOE observed 11-year temperature variations. For in-phase forcing, ocean mixed layer response lags surface air response by ~2 years, and is ~0.06 K compared to ~0.14 K for atmosphere. For out-of-phase forcing, lags are similar, but surface responses are significantly smaller. For both scenarios, modelE surface responses are less than 0.1 K in the tropics, and display similar patterns over oceanic regions, but complex responses over land. **Citation:** Cahalan, R. F., G. Wen, J. W. Harder, and P. Pilewskie (2010), Temperature responses to spectral solar variability on decadal time scales, *Geophys. Res. Lett.*, *37*, L07705, doi:10.1029/2009GL041898.

1. Introduction

[2] Solar forcing is the primary external forcing of Earth's climate. In order to fully understand the climate system one needs to have a better understanding of the climate response to this unique external forcing. Efforts have been made to reconstruct historical spectral solar irradiance (SSI) [e.g., *Lean*, 2000], to model the climate response to solar variations [e.g., *Rind et al.*, 1999; *Shindell et al.*, 1999; *Meehl et al.*, 2009], and to seek evidence for sun-climate connections from observations [e.g., *White*, 2006; *Camp and Tung*, 2007; *Lean and Rind*, 2008]. Modeling studies and empirical evidence together have connected solar variations with corresponding climate responses [*Haigh*, 2003]. Despite these advances, the role of solar forcing in climate change remains relatively poorly understood, compared for example to that of greenhouse gas forcing.

[3] Satellite observations over the past 30 years show that the total solar irradiance (TSI) changes with solar activity. The magnitude of change in TSI is about 0.1% over an 11-year solar cycle. However the change of TSI does not provide a complete description of solar variations, and is not sufficient for sun-climate studies. Total solar output energy consists of radiation of different wavelengths, with primary contributors to TSI ranging from ultraviolet (UV) to visible (VIS) and near infrared (NIR). The Earth's atmosphere and ocean respond differently to different wavelengths of solar radiation. The UV spectrum is responsible for stratospheric heating, and formation of the ozone layer. The VIS spectrum heats the ocean mixed layer and drives upper oceanic circulation. The NIR directly heats the troposphere by water vapor absorption. Thus the mechanisms by which solar irradiance varies at different wavelengths, and the corresponding mechanisms by which Earth's climate responds to such variations, are fundamental questions in sun-climate studies.

[4] Precise observations of variations in the UV spectrum of solar radiation began with the Upper Atmosphere Research Satellite (UARS) in 1991. However observations of the full SSI are not available until the launch of the Solar Radiation and Climate Experiment (SORCE) in January 2003. Although recent observations from SORCE have not yet completed a full solar cycle, solar variations that solar physicists and climate scientists did not fully anticipate have already been observed. For example, "the long-standing belief that the contributions of active regions to solar irradiance at wavelengths in the range of 1.2–3 μm is negative" is incorrect [*Fontenla et al.*, 2004]. Recently *Harder et al.* [2009] discovered that during the declining phase of solar cycle 23, SSI at one wavelength band has a multi-year trend out-of-phase with that of another band. Variations of SSI do not preserve the shape of the spectral distribution.

[5] As SORCE continues to make valuable TSI and SSI measurements, current available datasets may be used to provide possible scenarios and clues of long-term solar irradiance variations. The goal of this paper is not to provide definitive answers on how solar irradiance varies and how Earth's climate responds. Rather we study possible climate responses implied by the new observations, employing for that purpose a simple radiative-convective model (RCM) and also full GCM simulations, focusing on physical understanding of the responses.

[6] In section 2 we summarize SORCE observational evidence of the SSI variations that motivate this research. Section 3 describes the RCM and GCM climate models used in this research. Section 4 describes the model experiments with in-phase and out-of-phase SSI, and also presents the modeling results. Finally, section 5 summarizes results and conclusions.

2. Solar Spectral Forcing

[7] A major finding from SIM observations is that the temporal variation of SSI differs dramatically from what

[1]NASA Goddard Space Flight Center, Greenbelt, Maryland, USA.
[2]Goddard Earth Sciences and Technology Center, University of Maryland Baltimore County, Baltimore, Maryland, USA.
[3]Laboratory for Atmospheric and Space Physics, University of Colorado, Boulder, Colorado, USA.

0094-8276/10/2009GL041898

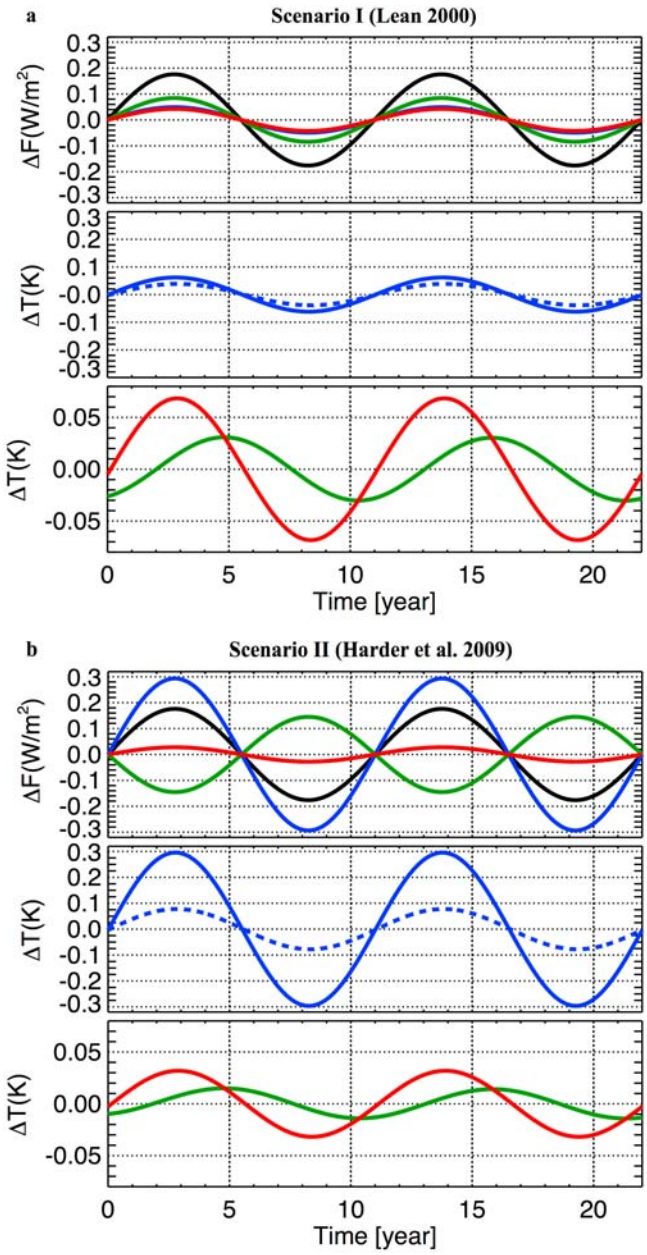

Figure 1. (a) TOA SSI forcing based on reconstructed SSI [*Lean*, 2000] with anomalies in TSI (black), UV at 200–400 nm (blue hidden by red in upper left panel), visible at 400–700 nm (green), and NIR 700–10000 nm (red) (top panel); stratospheric temperature response at 40 km (solid) and 25 km (dashed) (middle panel); the surface air temperature (red) and ocean mixed layer temperature (green) responses (bottom panel). (b) Similar to the Figure 1a, but for TOA SSI forcing based on SORCE SIM observations [*Harder et al.*, 2009].

was anticipated from SSI values reconstructed from proxies. By comparing SIM observations with reconstructed SSI from *Lean* [2000], *Harder et al.* [2009] show that both the observations and the reconstructed values have similar magnitude of variations in TSI. However the amplitude and even the phase of observed SSI variations are quite different from the reconstructions, except in one NIR band at 691–972 nm. Harder et al. show that on multi-year scales the SIM observed SSI of VIS and NIR bands varies out-of-phase with variations in the UV and TSI. In addition, the magnitude of decrease in UV band energy at 200–400 nm during the declining phase of solar cycle 23 is nearly 10 times as large as that for the reconstructed UV irradiance. In the VIS (400–691 nm), the SIM observed SSI changes out-of-phase with variations of TSI and reconstructed SSI. The magnitude of the increase of observed visible SSI is more than twice as large as the magnitude of the decrease of reconstructed SSI in the same spectral band. Similar out-of-phase variation with large amplitude is also evident for observed SSI in NIR band at 972–2423 nm [see *Harder et al.*, 2009].

[8] SORCE SIM observations span about $^1/_2$ of a solar 11-year cycle so far, but already these observations suggest that it is time for a re-examination of the impact of solar variation on climate. Here we examine the climate response to two scenarios of solar forcing. Scenario I is in-phase SSI variation based on the reconstructed SSI [*Lean*, 2000]. Scenario II is out-of-phase SSI variation based on the SIM observations [*Harder et al.*, 2009]. For simplicity we use simple sinusoids to describe successive 11-year solar variations for both in-phase and out-of-phase scenarios with amplitudes and phases given by *Harder et al.* [2009]. For both scenarios the amplitude of SSI are scaled to have 11-year TSI peak-to-peak variations of 1.2 W/m^2 (see identical black curves in top panels in Figure 1a and 1b). We also note that SIM covers the spectral range up to 2423 nm. SSI variations beyond SIM's wavelength upper limit are computed from the difference between the variation in TSI and SIM's observed SSI variations.

3. Model Descriptions

[9] We employ both the RCM and GISS modelE to study the climate response to the time and wavelength variations of solar radiation. We use the simple 1-dimensional (1D) RCM to estimate Earth's climate response to the two scenarios of SSI variations. Based on RCM results we further design experiments for modelE runs. Here we briefly describe RCMs and GISS modelE used in the present work.

3.1. Time-Dependent Radiative-Convective Model

[10] The radiative convective models have been widely used to perform climate sensitivity studies [e.g., *Manabe and Wetherald*, 1967; *Lindzen et al.*, 1982; *Arking*, 2005]. Here we extend the RCM to couple with an ocean mixed layer, and to include time dependence. For the atmosphere, we apply the lapse rate adjustment method [*Manabe and Wetherald*, 1967] to model the atmospheric convection and climate response. The RCM represents a given latitude zone, and we choose the latitude by setting the net incoming solar radiation at the top-of-the-atmosphere to 80 W/m^2 which is typical of the tropics [e.g. *Peixoto and Oort*, 1992, Figure 6.14d]. Radiation codes [*Chou*, 1992] are used to compute radiative heating rates and associated temperature changes. In the RCM, the atmosphere and the ocean-mixed layer are coupled through energy exchange and hydrological processes at the interface between the ocean-mixed layer

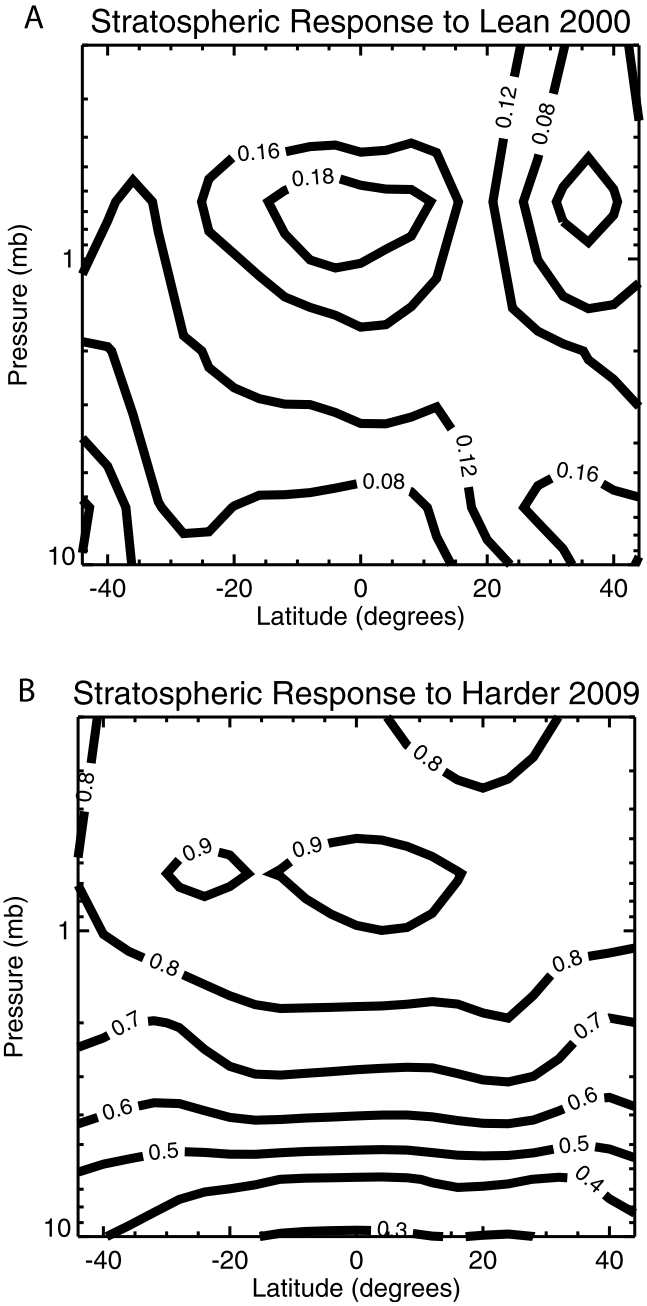

Figure 2. (a) The vertical profile of zonal average of the climate responses to the in-phase solar spectral forcing based on proxy reconstructed SSI [*Lean*, 2000]; (b) similar to Figure 2a, but for response to the out-of-phase solar spectral forcing based on SORCE [*Harder et al.*, 2009].

and the atmosphere. The ocean mixed layer temperature is governed by

$$\rho_w C_w H_m \frac{dT_m(t)}{dt} = -\rho_a \cdot C_D \cdot V\{L[q_s(T_m(t)) - q(T_s(t))] + C_p[T_m(t) - T_s(t)]\} + F_r(t) \quad (1)$$

where is ρ_w water density, C_w the specific heat of water, H_m the depth of ocean mixed layer, T_m the mixed layer temperature, ρ_a the air density, C_D the drag coefficient, V the surface wind speed, L the latent heat of vaporization, q_m the saturation mixing ratio at temperature T_m, q_s the mixing ratio in the atmospheric surface layer, C_p the specific heat of air, T_s the surface air temperature, and F_r the surface net radiation flux. An increase or decrease of the mixed layer temperature (left hand side of equation (1)) is a result of gaining or losing energy (right hand side of equation (1)). Typical values for parameters in equation (1) are specified as $C_D = 0.0014$, $H_m = 63$m, $V = 5$ m/s.

3.2. GISS ModelE

[11] The RCM provides a first estimate of climate response to solar variations and aids GCM experimental design. The GISS modelE is the latest incarnation of the GISS series of coupled atmosphere-ocean models. The GISS GCM has been used in sun-climate studies [e.g., *Rind et al.*, 1999; *Shindell et al.*, 1999]. The atmospheric model used in this study is the 20-layer version of the modelE. The model has a horizontal resolution of 4° (latitude) × 5° (longitude). The model top is at 0.1 hPa or ~65 km above sea surface. The three-dimensional atmospheric general circulation model is coupled with a simplified thermodynamic ocean model - the Q-flux ocean model. The Q-flux model allows the SST to adjust to different atmospheric fluxes, but holds the ocean transports constant. The ocean heat convergence (the Q-fluxes) into the isothermal mixed layer is computed as a residual, given by the heat and mass fluxes at the base of the atmosphere, and observed mixed layer temperature and depth. Details of GISS modelE are described by *Schmidt et al.* [2006].

[12] Transient climate responses to the two solar forcing scenarios are simulated with modelE. The simulation runs for 105 years, with greenhouse gases fixed at present values. To reduce noise due to natural variability, we average temperatures over individual years during solar maximum and solar minimum. Temperature differences between solar maximum and solar minimum provide a measure of climate response to the 11-year cycle of solar variations.

4. Results

[13] The two scenarios of solar forcing described in section 2 are applied to the RCM and GISS modelE to study the climate response. The results for RCM and GISS modelE simulations are presented below.

4.1. RCM Results

[14] The assumed forcing of SSI and the associated responses of atmospheric and ocean mixed layer temperatures computed from the RCM are presented in Figure 1.

[15] The variations in TSI are the same for both scenarios (black curves in top panels of Figure 1a and 1b). However, the SSI forcings in the two scenarios are quite different from each other (colored curves in top panels of Figure 1a and 1b). For scenario I, the SSI at all wavelengths varies in-phase with the TSI. However, for scenario II not all SSI bands vary in-phase with the TSI. For scenario II, the SSI in the UV varies in phase with TSI, but with an amplitude about 10 times larger than that for scenario I; the SSI in the visible band varies out-of-phase with TSI, with a amplitude about twice as large as that for scenario I; the SSI in the NIR band varies in phase with TSI, with a amplitude about the same as that for scenario I.

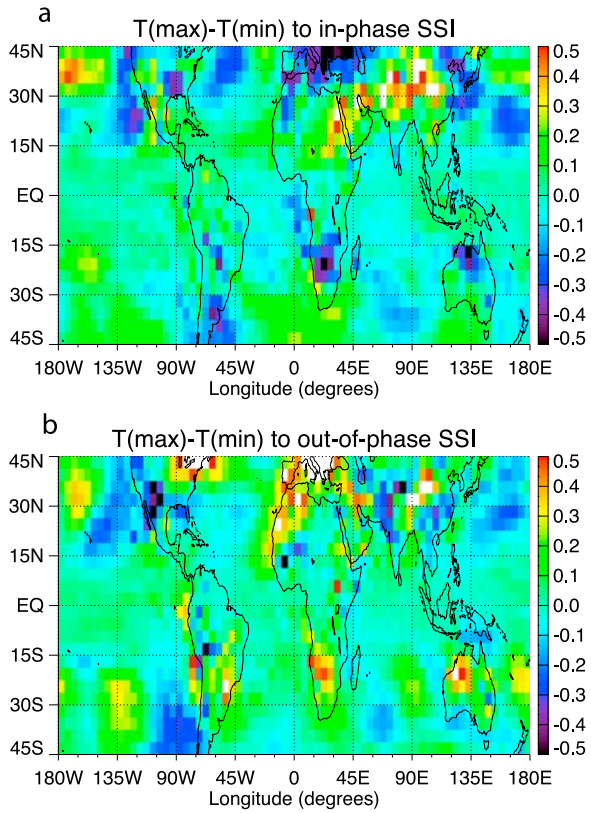

Figure 3. (a) Responses of surface air temperature to the in-phase SSI forcing. (b) Responses of surface air temperature to the out-of-phase SSI forcing.

[16] The climate has very different responses to the two different scenarios of SSI forcing. In the upper stratosphere at ~40 km, the peak-to-peak variation of temperature in the upper stratosphere is about 0.6 K for scenario II, which is about 6 times as large as that for scenario I (see middle panels in Figure 1a and 1b). The stratospheric temperature responses for both scenarios are in phase with the TOA UV spectral irradiance, that varies in phase with TSI. The temperature responses decrease downward for both scenarios. The surface temperature response of scenario I forcing is much larger as compared to that of scenario II forcing (see bottom panels in Figure 1a and 1b). For scenario I, the peak-to-peak variation of surface air temperature is about 0.14 K as compared to the 0.08 K in scenario II. Ocean mixed layer response is about half as large as the surface atmosphere response. It is important to note that the surface air response lags by ~1 month to the TSI variation, and the ocean mixed layer response lags the atmosphere response by ~2 years for both scenarios.

4.2. GISS ModelE Results

[17] The GCM simulations also show different climate responses to the two different scenarios of SSI forcing. Figure 2 shows the profiles of the zonal mean of the stratospheric response to the two forcing scenarios. It is evident that the maximum stratospheric temperature response occurs in the upper stratosphere near 1 hPa or ~48 km over the tropics, and the amplitude of the response decreases downwards for both solar forcing scenarios. However the amplitude of the maximum temperature response to out-of-phase solar forcing is about 1 K, and is about 5 times larger than the response to the in-phase solar forcing, similar to what was found in the RCM.

[18] The surface temperature responses to the in-phase and out-of-phase SSI forcings are presented in Figure 3. The surface responses to the two scenarios of SSI forcing have similarities and differences. Over the tropical oceans, the surface air temperature responses are similar for the two forcing scenarios, with amplitude of temperature change about 0.1 K. Negative responses are found off the coast of California, over North Pacific Ocean, and South Indian Ocean. A negative response off the coast of Chile is found for the out-of-phase Scenario II as compared to a similar response about 30 degrees eastwards for the in-phase Scenario I. The responses over land are complex, even with different sign for the two scenarios. The global average surface air temperature of solar max minus solar min is ~0.004 K for scenario I; and is ~0.05 K for scenario II. In the tropical region in 20°S–20°N, the zonal average surface air temperature of solar max minus solar min is ~0.002 K for scenario I; and is about 0.02 K for scenario II.

5. Summary and Discussion

[19] We use (I) proxy-based in-phase and (II) SIM observation-based out-of-phase SSI forcing to drive an RCM and GISS modelE. For both SSI forcing scenarios, we found that maximum temperature responses occur in upper stratosphere, decreasing downward. Maximum stratospheric temperature response to SIM-based Scenario II is about 0.6 K for RCM and 1 K for modelE in the tropics, and is about 5–6 times larger than responses to proxy-based solar forcing. Stratospheric temperature responses to the SIM-based forcing is consistent with the observed 11-year upper stratospheric temperature response from HALOE [*Remsberg*, 2008]. Although modeled solar cycle temperature responses are similar to HALOE observations at low latitudes, their respective responses are not as similar at middle latitudes. This difference may arise from dynamical effects not included in the 20-layer version of GISS modelE.

[20] Surface temperature responses in the RCM are about an order of magnitude smaller than upper stratospheric responses. We find surface atmospheric response ~1 K, about twice as large as the mixed layer response. The surface air response lags the TSI variation by ~1 month, while the ocean mixed layer response lags the surface air response by ~2 years for both in-phase and out-of-phase SSI forcings. Surface atmospheric responses are ~0.14 K and ~0.08 K for the in-phase and out-of-phase SSI forcing, respectively. The surface response is consistent with the observed solar signal from a robust multivariate analysis [*Lean and Rind*, 2008]. Our result also suggests that computed 11-year amplitudes of 0.2 K [*Camp and Tung*, 2007] and 0.3 K [*White,* 2006] are not likely solar only, but may well include other climate signals that contribute to temperature variations on the 11-year timescale.

[21] Since the RCM does not include chemistry, to mimic in the ozone variations observed in the RCM, we consider the impact of a 1% peak-to-peak ozone change. For scenario I, we find temperature response increase to ~0.28 K and ~0.3 K for the upper and lower stratosphere, respectively; while for scenario II, temperature response increases to

0.68 K and 0.26 K for the upper and lower stratosphere, respectively. So the assumed 1% ozone change has observable impacts on stratospheric temperature responses. However, we find no significant surface temperature response to the assumed 1% ozone change in the RCM.

[22] In the modelE simulations, we found different spatial patterns for the two SSI forcing inputs. Over the tropical oceans, the surface air temperature responses to the two SSI forcings are similar, with peak-to-peak temperature change about 0.1 K. We also found negative responses over some ocean regions. The simulations show complex responses over land. The global average surface air temperature of solar max minus solar min is ~0.004 K for scenario I; and is ~0.05 K for scenario II. In the tropical region 20°S–20°N, the zonal average surface air temperature of solar max minus solar min is ~0.002 K for in-phase Scenario I forcing; and is about 0.02K for out-of-phase Scenario II. These surface responses are too small to be easily observed.

[23] This study focuses on the temperature response to spectral in-phase versus out-of-phase decadal variations in SSI. Of course, temperature is not the only climate indicator, and the time scale of climate variations is not only decadal, but also spans centennial and longer periods. Solar activity varies on centennial time scales, as indicated by sunspot variations since the Maunder Minimum in sunspot number. At the same time as these centennial variations of external solar forcing, there are also variations of internal forcing due to increases of greenhouse gases, and changes of aerosol loading due to volcanic and other natural variations, as well as changes in human activities. Further research is required to reassess the climate responses to each of these forcings on centennial time scales given the new SSI observations. The research should be extended to include direct and indirect impacts of solar forcing associated with variations in SSI. The research should also be extended to study associated changes in precipitation on global and regional scales. Here we used a simplified RCM to perform the first estimate of temperature responses, and to design experiments for GCM simulations. With the GISS modelE as a laboratory for climate research, and with continuing satellite observations of SSI variations, we anticipate continued advances in understanding sun-climate connections.

[24] **Acknowledgments.** This research was supported by NASA's Living With a Star program, thanks to Program Manager M. Guhathakurta. We also thank A. Arking, J. Lean, W. Ridgway, and D. Rind for helpful discussions.

References

Arking, A. (2005), Effects of bias in solar radiative transfer codes on global climate model simulations, *Geophys. Res. Lett.*, *32*, L20717, doi:10.1029/2005GL023644.

Camp, C. D., and K. K. Tung (2007), Surface warming by the solar cycle as revealed by the composite mean difference projection, *Geophys. Res. Lett.*, *34*, L14703, doi:10.1029/2007GL030207.

Chou, M.-D. (1992), A solar radiation model for use in climate studies, *J. Atmos. Sci.*, *49*(9), doi:10.1175/1520-0469(1992)049<0762:ASRMFU>2.0.CO;2.

Fontenla, J. M., J. Harder, G. Rottman, T. N. Woods, G. M. Lawrence, and S. Davis (2004), The Signature of Solar Activity in the Infrared Spectral Irradiance, *Astrophys. J.*, *605*, L85, doi:10.1086/386335.

Haigh, J. D. (2003), The effects of solar variability on the Earth's climate, *Philos. Trans. R. Soc. London, Ser. A*, *361*, 95–111, doi:10.1098/rsta.2002.1111.

Harder, J. W., J. M. Fontenla, P. Pilewskie, E. C. Richard, and T. N. Woods (2009), Trends in solar spectral irradiance variability in the visible and infrared, *Geophys. Res. Lett.*, *36*, L07801, doi:10.1029/2008GL036797.

Lean, J. (2000), Evolution of the Sun's spectral irradiance since the Maunder Minimum, *Geophys. Res. Lett.*, *27*(16), 2425–2428, doi:10.1029/2000GL000043.

Lean, J. L., and D. H. Rind (2008), How natural and anthropogenic influences alter global and regional surface temperatures: 1889 to 2006, *Geophys. Res. Lett.*, *35*, L18701, doi:10.1029/2008GL034864.

Lindzen, R. S., A. Y. Hou, and B. F. Farrell (1982), The role of convective model choice in calculating the climate impact of doubling CO_2, *J. Atmos. Sci.*, *39*, 1189–1205, doi:10.1175/1520-0469(1982)039<1189:TROCMC>2.0.CO;2.

Manabe, S., and R. Wetherald (1967), Thermal equilibrium of the atmosphere with a given distribution of relative humidity, *J. Atmos. Sci.*, *24*(3), 241–259, doi:10.1175/1520-0469(1967)024<0241:TEOTAW>2.0.CO;2.

Meehl, G. A., J. M. Arblaster, K. Matthes, F. Sassi, and H. van Loon (2009), Amplifying the Pacific climate system response to a small 11 year solar cycle forcing, *Science*, *325*, 1114–1118, doi:10.1126/science.1172872.

Peixoto, J. P., and A. H. Oort (1992), *Physics of Climate*, 520 pp., Am. Inst. of Phys., New York.

Remsberg, E. E. (2008), On the response of Halogen Occultation Experiment (HALOE) stratospheric ozone and temperature to the 11-year solar cycle forcing, *J. Geophys. Res.*, *113*, D22304, doi:10.1029/2008JD010189.

Rind, D., J. Lean, and R. Healy (1999), Simulated time-dependent climate response to solar radiative forcing since 1600, *J. Geophys. Res.*, *104*, 1973–1990, doi:10.1029/1998JD200020.

Schmidt, G. A., et al. (2006), Present day atmospheric simulations using GISS ModelE: Comparison to in-situ, satellite and reanalysis data, *J. Clim.*, *19*, 153–192, doi:10.1175/JCLI3612.1.

Shindell, D., D. Rind, N. Balachandran, J. Lean, and P. Lonergan (1999), Solar cycle variability, ozone, and climate, *Science*, *284*, 305–308, doi:10.1126/science.284.5412.305.

White, W. B. (2006), Response of tropical global ocean temperature to Sun's quasi-decadal UV radiative forcing of the stratosphere, *J. Geophys. Res.*, *111*, C09020, doi:10.1029/2004JC002552.

R. F. Cahalan and G. Wen, NASA Goddard Space Flight Center, Code 613.2, Greenbelt, MD 20771, USA. (guoyong.wen-1@nasa.gov)

J. W. Harder and P. Pilewskie, Laboratory for Atmospheric and Space Physics, University of Colorado, Boulder, CO 80309-0392, USA.